Author Index

Aust, K. T., 157 Austin, M. W., 85

Bhattacharya, R. S., 139 Boas, M., 77 Budhani, R. C., 165 Bunshah, R. F., 165

Casalot, A., L9 Charsely, P., 101 Chaturvedi, M. C., 59 Collot, J., L5 Combres, Y., L5

Dal Maschio, R., L25 Demsetz, L. A., 33 Deshpandey, C. V., 165 Doerr, H. J., 165

Ficalora, P. J., 43

Gibson, L. J., 33 Gnanam, F. D., L1 Goswami, N. N., 147 Gupta, H. C., 187

Han, Y., 59

Kelly, A., 1 Kim, S. A., 85 Korhonen, A. S., L19 Kunz, L., 67 Kurzydlowski, K. J., 115

Lal, K., 147 Ledbetter, H. M., 85 Lukáš, P., 67

Mackay, R. A., 127 Malhotra, J., 187 Me-Bar, Y., 77 Molarius, J. M., L19 Mughrabi, H., 15

Nathal, M. V., 127

Palaniappan, L., L1 Prakashi, S., 165

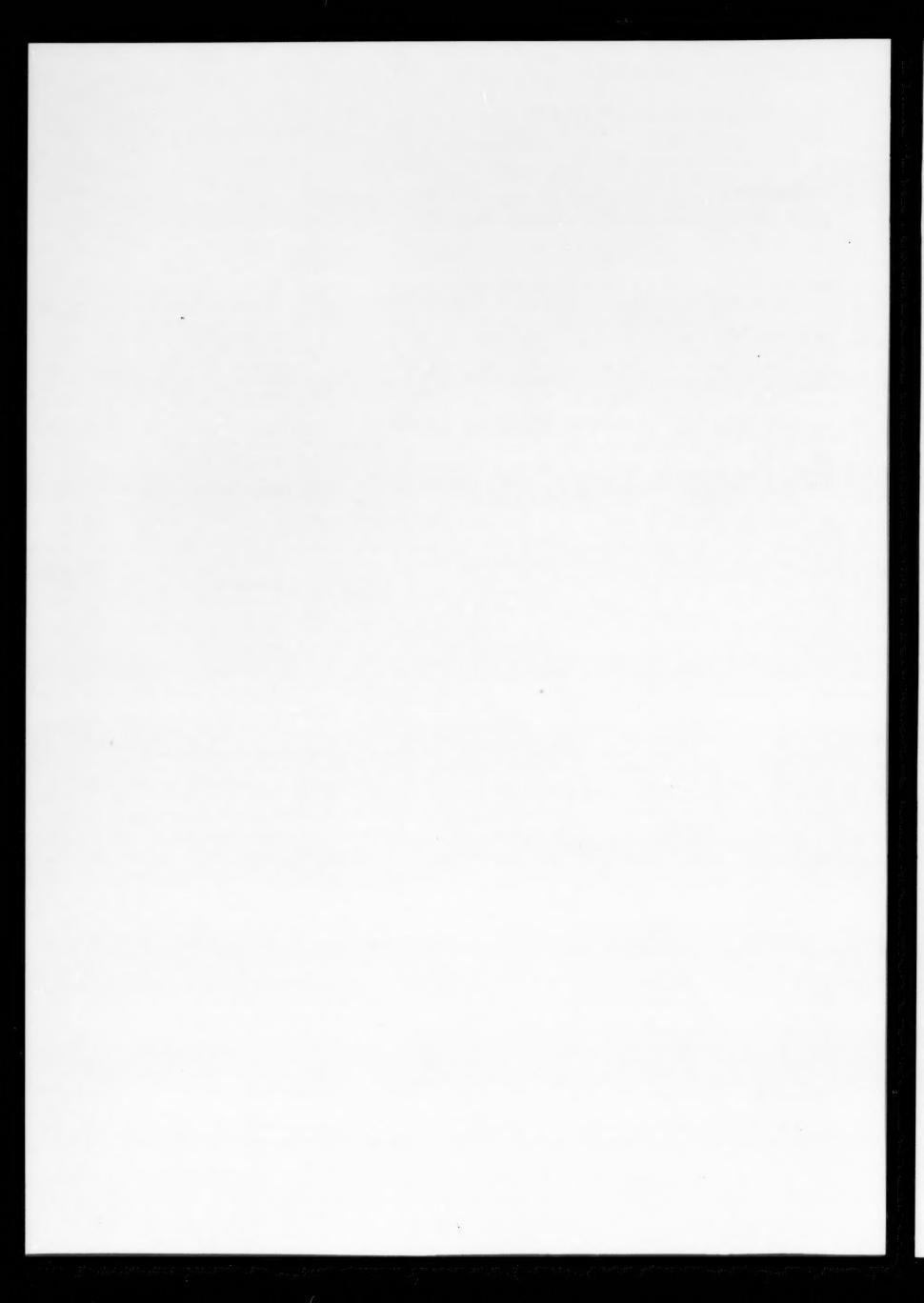
Rai, A. K., 139 Ramasamy, P., L1 Rani, N., 187 Rodríguez, M. V., 43 Rosenberg, Z., 77

Savva, G., 157 Smith, E., 53 Sorarù, G., L25

Tangri, K., 115 Tripathi, B. B., 187

Vacquier, G., L9 Varin, R. A., 115

Waseda, Y., 157 Wetherhold, R. C., L13 White, J. D. M., 101 Whittenberger, J. D., 91 Wriekat, A., 181



Subject Index

Alloy

the torsion behaviour of stir-cast Cu-11wt.%Sn alloy at room temperature, L5

Aluminium

effects of pretreatments on the oxidation behaviour of Ni-Co-Cr-Al-Y coatings, 165

slow plastic flow properties of B2 Co-Fe-Al and Co-Ni-Al between 1100 and 1400K, 91 spall studies on Ti-6Al-4V, 77

Antimony sulphoiodide

electrical conductivity of antimony sulphoiodide, L1

Auger electron spectroscopy

superficial characterization of NbSe₂ single crystals: an Auger electron spectroscopy study, L9

Boron

corrosion of Fe-Cr-Si-B metallic glass wires, 157

Carbon

carbon and nitrogen effects on the elastic constants of a stainless steel at 4K, 85

Chromium

corrosion of Fe-Cr-Si-B metallic glass wires, 157 effects of pretreatments on the oxidation behaviour of Ni-Co-Cr-Al-Y coatings, 165 sputter-deposited and ion-mixed Ni-Ti and Ni-Cr thin films, 139

Coatings

effects of pretreatments on the oxidation behaviour of Ni-Co-Cr-Al-Y coatings, 165

Cobalt

effects of pretreatments on the oxidation behaviour of Ni-Co-Cr-Al-Y coatings, 165

slow plastic flow properties of B2 Co-Fe-Al and Co-Ni-Al between 1100 and 1400K, 91

Conductivity

electrical conductivity of antimony sulphoiodide,

Copper

deformation during fatigue near surface identations and pits in copper crystals, 101

effect of grain size on the high cycle fatigue behaviour of polycrystalline copper, 67

the torsion behaviour of stir-cast Cu-11wt.%Sn alloy at room temperature, L5

Cores

minimum weight design for stiffness in sandwich plates with rigid foam cores, 33

Crack

the effective fracture energy associated with cleavage crack growth in B.C.C. iron, 53

Creep

a study of back stress during creep deformation of a superalloy Inconel 718, 59 Crystals

superficial characterization of NbSe₂ single crystals: an Auger electron spectroscopy study, L9

Deformation

a study of back stress during creep deformation of a superalloy Inconel 718, 59

deformation during fatigue near surface indentations and pits in copper crystals, 101

Dislocation

a two-parameter description of heterogeneous dislocation distributions in deformed metal crystals, 15

analytical treatment of grain boundary sources for dislocations, 115

the mechanism of a hydrogen-dislocation interaction in B.C.C. metals: Embrittlement and dislocation motion, 43

Ductility

ductility of TiN-coated high speed steel, L19

Elastic

carbon and nitrogen effects on the elastic constants of a stainless steel at 4K, 85

Embrittlement

the mechanism of a hydrogen-dislocation interaction in B.C.C. metals: Embrittlement and dislocation motion, 43

Fatigue

deformation during fatigue near surface identations and pits in copper crystals, 101

effect of grain size on the high cycle fatigue behaviour of polycrystalline copper, 67

influence of surface treatments on the dynamic fatigue of soda-lime glass with identation flaws, L25

Films

sputter-deposited and ion-mixed Ni-Ti and Ni-Cr thin films, 139

Flaws

influence of surface treatments on the dynamic fatigue of soda-lime glass with identation flaws, L25

Fracture

the effective fracture energy associated with cleavage crack growth in B.C.C. iron, 53

Grain boundary

analytical treatment of grain boundary sources for dislocations, 115

Graphite

phonons in graphite and LiC₆, 187

Hydrogen-dislocation interaction the mechanism of a hydrogen-dislocation inter-

action in B.C.C. metals: Embrittlement and dislocation motion, 43

Iron

corrosion of Fe-Cr-Si-B metallic glass wires, 157 slow plastic flow properties of B2 Co-Fe-Al and Co-Ni-Al between 1100 and 1400K, 91 the effective fracture energy associated with cleavage crack growth in B.C.C. iron, 53

Lamellar γ - γ' structures the stability of lamellar γ - γ' structures, 127 Lithium carbide phonons in graphite and LiC₆, 187

Materials science

an outline of trends in materials science and processing, 1

Metals

the mechanism of a hydrogen-dislocation interaction in B.C.C. metals: Embrittlement and dislocation motion, 43

surface analysis of light elements at metal surfaces using (p, γ) reactions, 181

Metal Crystals

a two-parameter description of heterogeneous dislocation distributions in deformed metal crystals, 15

Metallic glass wires corrosion of Fe-Cr-Si-B metallic glass wires, 157

Nickel

effects of pretreatments on the oxidation behaviour of Ni-Co-Cr-Al-Y coatings, 165
slow plastic flow properties of B2 Co-Fe-Al and
Co-Ni-Al between 1100 and 1400K, 91
sputter-deposited and ion-mixed Ni-Ti and Ni-Cr
thin films, 139

Niobium

superficial characterization of NbSe₂ single crystals: an Auger electron spectroscopy study, L9

carbon and nitrogen effects on the elastic constants of a stainless steel at 4K, 85 ductility of TiN-coated high speed steel, L19

 (p, γ) reactions

surface analysis of light elements at metal surfaces using (p, γ) reactions, 181

Phonons

phonons in graphite and LiC6, 187

Plastic

slow plastic flow properties of B2 Co-Fe-Al and Co-Ni-Al between 1100 and 1400K, 91

Sandwich plates

minimum weight design for stiffness in sandwich plates with rigid foam cores, 33

Selenium

superficial characterization of NbSe₂ single crystals: an Auger electron spectroscopy study, L9

Silicon

corrosion of Fe-Cr-Si-B metallic glass wires, 157 high resolution X-ray diffraction study of defect structures produced by high D.C. electric fields in silicon single crystals, 147

Soda-lime glass

influence of surface treatments on the dynamic fatigue of soda-lime glass with indentation flaws, L25

Spall

spall studies on Ti-6Al-4V, 77

Stainless steel

carbon and nitrogen effects on the elastic constants of a stainless steel at 4K, 85

Steel

ductility of TiN-coated high speed steel, L19
Stress

a study of back stress during creep deformation of a superalloy Inconel 718, 59

Superalloy

a study of back stress during creep deformation of a superalloy Inconel 718, 59 deformation of surface cladding and matrix of

deformation of surface cladding and matrix of tungsten-fiber-reinforced superalloy under thermomechanical loading, L13

Thermomechanical loading

deformation of surface cladding and matrix of tungsten-fiber-reinforced superalloy under thermomechanical loading, L13

Tin

the torsion behaviour of stir-cast Cu-11wt.%Sn alloy at room temperature, L5

Titanium

ductility of TiN-coated high speed steel, L19 spall studies on Ti-6Al-4V, 77 sputter-deposited and ion-mixed Ni-Ti and Ni-Cr thin films, 139

Torsion

the torsion behaviour of stir-cast Cu-11wt.%Sn alloy at room temperature, L5

Tungsten

deformation of surface cladding and matrix of tungsten-fiber-reinforced superalloy under thermomechanical loading, L13

Vanadium

spall studies on Ti-6Al-4V, 77

X-ray diffraction

high resolution X-ray diffraction study of defect structures produced by high D.C. electric fields in silicon single crystals, 147

Yttrium

effects of pretreatments on the oxidation behaviour of Ni-Co-Cr-Al-Y coatings, 165

